Published in final edited form as:
Magn Reson Imaging. 2013 July ; 31(6): 1017–1021. doi:10.1016/j.mri.2013.03.007.

Intra-Voxel Incoherent Motion MRI in Rodent Model of Diethylnitrosamine-Induced Liver Fibrosis

Yue Zhang, M.S.[1,2], **Ning Jin, Ph.D.**[3], **Jie Deng, Ph.D.**[4], **Yang Guo, M.D.**[2], **Sarah B. White, M.D.**[2,5], **Guang-Yu Yang, M.D., Ph.D.**[5,6], **Reed A. Omary, M.D., M.S.**[2,5,7], and **Andrew C. Larson, Ph.D.**[1,2,5,7]

[1]Department of Bioengineering, University of Illinois at Chicago, Chicago, IL

[2]Department of Radiology, Northwestern University, Chicago, IL

[3]Siemens Healthcare, Columbus, OH

[4]Department of Medical Imaging, Lurie Children's Hospital of Chicago, Chicago, IL

[5]Department of Radiology, Medical College of Wisconsin, Milwaukee, WI

[5]Robert H. Lurie Comprehensive Cancer Center, Chicago, IL

[6]Department of Pathology, Northwestern University, Chicago, IL

[7]Department of Biomedical Engineering, Northwestern University, Evanston, IL

Abstract

Rationale and Objectives—To compare the apparent diffusion coefficient (*ADC*) and the perfusion fraction measured by intra-voxel incoherent motion (IVIM) Magnetic Resonance Imaging (MRI) with liver fibrosis degrees in a rodent model.

Materials and Methods—All experiments received approval from our institutional animal care and use committee. Liver fibrosis was induced in 17 rats by oral gavage with diethylnitrosamine. Diffusion Weighted MRI was the performed and 8 gradient factors (0, 50, 100, 150, 200, 300, 400 and 500 sec/mm^2) were acquired. The values of *ADC*, true diffusion coefficient *D* and perfusion fraction *f* were measured based on Li Bihan's method. The percentage of liver fibrosis was assessed via quantitative analysis of Masson trichrome staining using an average of 30 fields per section. The MRI measurements were compared to the histological fibrotic grade to evaluate the correlation between them.

Results—*ADC* contained the contribution of diffusion and perfusion. The *ADC* and *f* values decreased significantly with the increasing fibrosis level (correlation coefficient: *ADC*: $\rho = -0.781$, $p < 0.001$; *f*: $\rho = -0.720$, $p = 0.001$); but *D* was poorly correlated with fibrosis level ($\rho = -0.502$, $p = 0.040$).

Conclusion—The hepatic ADC and the perfusion fraction *f* were significantly correlated with the liver fibrosis level; however, D was not. This might suggest that hepatic perfusion is altered during the progression of hepatic fibrosis.

Please send proof and correspondence to: Andrew C. Larson, Ph.D., Department of Radiology, Northwestern University, 737 N. Michigan Ave, Suite 1600, Chicago, IL 60611, USA, Tel: (312) 926-3499 Fax: (312)926-5991, a-larson@northwestern.edu.

Keywords

Intra-Voxel Incoherent Motion; Diffusion weighted MRI; liver fibrosis

INTRODUCTION

Liver fibrosis is the result of chronic hepatic tissue deconstruction, such as the accumulation of tough, fibrotic scar tissue in the liver (1, 2). It can be caused by alcoholic liver disease(3), chronic hepatitis B(4) or chronic hepatitis C(5), among other causes. The gold standard for the diagnosis of liver fibrosis is invasive liver biopsy(6), which has a high associated morbidity. Liver biopsies also only give us an understanding of disease at the site of the biopsy, which may not correlate with the global function of the liver(7). Therefore, clinicians are seeking to find new ways to non-invasively determine the grade of fibrosis. Recently diffusion-weighted (DW) magnetic resonance imaging (MRI) has been considered as a potential tool to noninvasively detect liver fibrosis (8, 9). DW imaging is especially useful, in that no contrast is required, which in some patients is contraindicated due to their poor underlying renal function.

Conventional DW-MRI apparent diffusion coefficient (ADC) measurements integrate the contribution of both diffusion and perfusion components (10, 11). DW intra-voxel incoherent motion (IVIM) imaging permits in vivo quantification of the microscopic translational motion of water that occurs due to molecular diffusion and/or microcirculation of blood within capillary networks (perfusion)(10, 12). IVIM can be further analyzed as diffusion, which arises from the Brownian motion of individual molecules moving with large random thermal velocities, and perfusion, which describes the pseudorandom flow at low velocities of blood moving along the finely divided structures of the capillaries.

Recent studies showed that hepatic perfusion is decreased in fibrotic subjects compared with healthy ones (13, 14). During previous studies in the CCl_4 rodent model(15), decreases in liver ADC levels were well correlated to increased liver fibrosis. This inverse correlation was explained by the authors as a decrease in ADC caused by a decrease in perfusion given that ADC incorporates effects of both diffusion and perfusion (10). Recent clinical studies suggest that IVIM approaches offer the potential to differentiate the contributions of perfusion and water mobility during DW signal decay measurements in the liver(14, 16, 17).

The purpose of our study is to investigate the relationship between hepatic DW-IVIM measurements and diethylnitrosamine (DEN) -induced fibrosis levels in a Wistar rat model. Our hypothesis is that IVIM perfusion fraction measurements are inversely correlated to increased hepatic fibrosis degrees.

MATERIALS AND METHODS

Animal Model

All experiments were approved by our institutional animal care and use committee. Seventeen adult male Wistar rats (Harlan, Indianapolis, IN) weighting 350 – 400g were used for these experiments. DEN-induced liver fibrosis model in rodent has been well established for over 40 years and demonstrated DEN in rats with appropriate dose can simply induce hepatic fibrosis, cirrhosis or cancers that are suitable for a variety of tests (18). Liver fibrosis was induced in thirteen rats by oral gavage once a week with 5 mL/kg dose of 1.5% DEN solution (DEN ISOPAC®, Sigma Chemical, St Louis, MO). Four untreated rats were used as controls.

MRI Measurements

All experiments were performed using a 3.0T clinical MR scanner (Magnetom Trio, Siemens Medical Solutions, Erlangen, Germany) with a custom-built rodent receiver coil (Chenguang Medical Technologies Co., Shanghai, China). Imaging was performed for two rats on weeks 4, 5, 6, 7, for one rat on weeks 9 and 10 and for three rats on week 8 of DEN administration. Prior to imaging, rats were anesthetized with an intra-muscular injection of ketamine (80mg/mL, Ketaset; Fort Dodge Animal Health, Fort Dodge, Iowa) and xylazine (10mg/mL, Isothesia; Abbott Laboratories, North Chicago, IL). The abdomen of each rat was fixed with a belt of adhesive tape to limit respiratory motion. Coronal and transverse T2-weighted TSE images of the entire liver were acquired for localization. Axial IVIM scans were performed using a DW EPI sequence with the following imaging parameters: TR/TE=3500/71ms, 1260kHz/pixel bandwidth, 5/8 partial Fourier, EPI factor = 52, 4 signal averages, 3mm slice thickness, 150×61 mm^2 FOV, 52×128 matrix (1.2 × 1.2 × 3 mm^3 voxel size), and fat-sat preparation. Imaging was performed during free-breathing with respiratory belt triggering at expiration. DW images were acquired with gradient factors b = 0, 50, 100, 150, 200, 300, 400 and 500 sec/mm^2. Higher b values were not employed due to limited signal to noise ratio at high b values in this small animal study.

Imaging Analysis

Data analysis was performed offline using MATLAB software. Based on IVIM theory, DW signal attenuation is described by the following equation (10, 11):

$$\frac{SI_b}{SI_0}=(1-f)\times e^{-bD}+f\times e^{-bD^*}, \quad (1)$$

where D and D^* are the true diffusion coefficient and the pseudo-diffusion coefficient, respectively, and f is the perfusion fraction (fractional volume of the voxel occupied by the flowing spins), SI_b signifies the measured signal intensity for a given b value and SI_0 represents the signal intensity when b=0.

A nonlinear fitting for all parameters in Equation (1) simultaneously can be challenged by low SNR or limited fitting points (19, 20). Instead, we employed a stepwise strategy to determine D and f, similar to prior studies (19, 21–23). When DW gradient strengths were sufficiently strong, diffusion measurements began to approximate the true diffusion coefficient D. Hence first step, for each slice position, diffusion (D) maps were reconstructed on a voxel-by-voxel basis by fitting larger b values (b=150, 200, 300, 400 and 500 sec/mm^2) and corresponding signal intensities to the function: $-b\cdot D=\log(SI_b/SI_0)$. Second step, by substituting the D value generated in the first step into Equation (1), perfusion fraction (f) maps were reconstructed voxel-by-voxel by fitting all 8 b values and corresponding signal intensities to Equation (1). ADC maps were reconstructed for each slice position on a voxel-by-voxel basis by fitting all 8 b values and corresponding voxel signal intensities to the function: $-b\cdot ADC=\log(SI_b/SI_0)$. The region of interest (ROI) within the liver parenchyma was drawn for each slice on b=0 sec/mm^2 image (avoiding blood vessels) and these ROIs were transferred to the corresponding IVIM functional maps for mean ADC, D and f measurements in each animal.

Histological Analysis

Following each imaging study, animals were euthanized by intraveneous injection of pentobarbital and phenytoin sodium solution (150mg/kg); rat livers were harvested for histological evaluation: three slices were excised from the left lateral lobe (large lobe partially covered by the stomach), right lateral lobe (located under the medium lobe), and medium lateral liver lobe (located at the top of the liver with an obvious central cleft)(24)

from each rat. Liver specimens were fixed in 10% buffered formalin and paraffin embedded. Masson trichrome staining was used to identify collagen tissues. Histological slides were digitized with 200x optical magnification using a multi-channel image acquisition system (TissueGnostics, Vienna, Austria). A quantitative assessment of liver fibrosis was performed to describe the total percentage of fibrotic parenchyma area(25). The level of liver fibrosis was quantitatively measured by performing an average of 30 fields per section. The fibrosis region was measured by extracting the area of blue component (fibrosis was stained as blue within the Tri-chrome staining) by using ImageJ software (ImageJ 1.42o, National Institutes of Health, Bethesda, MD). The fibrosis level was expressed as the ratio between stained blue fibrotic tissue and total measured area. Specimens were evaluated by an experienced attending surgical pathologist with specialization in gastrointestinal oncology.

Statistical Analysis

All statistics were performed using SPSS (SPSS 11.0, Chicago, IL, USA). The Spearman's correlation coefficient was calculated to assess the correlation between the percent of liver fibrosis and *ADC*, *D*, and *f* levels. Tests were considered statistically significant when *p*-value < 0.05.

RESULTS

Histological liver specimens from the healthy control and the DEN-induced fibrosis rats were strikingly different on microscopic examination (Fig. 1). Blue regions in Fig.1b indicate a significant level of fibrosis in the DEN Rat. The values for perfusion fraction *f*, *ADC* and *D* are plotted against percent fibrosis level in Fig. 2. Both *ADC* (Fig. 2a) and perfusion fraction *f* (Fig. 2c) measurements were significantly correlated (inversely) with the fibrosis levels (*ADC*: $\rho = -0.781$, $p < 0.001$; *f*: $\rho = -0.720$, $p = 0.001$), while *D* (Fig. 2b) was poorly correlated ($\rho = -0.502$, $p = 0.040$). Representative *ADC*, *D* and *f* maps for three animals with different fibrosis levels (0%, 10.48% and 16.49%) were shown in Fig.3. We can visualize that the hepatic *ADC* and *f* values of 0% fibrosis (brighter on *ADC* and *f* maps) were higher than that of 10.48% and 16.49% fibrosis (darker on *ADC* and *f* maps), while hepatic *D* values were similar in the three levels of fibrosis.

Discussion

Our study successfully demonstrated the potential to use IVIM MRI measurements to correlate liver *ADC* and perfusion fraction to fibrosis level during disease progression. Decreasing perfusion fraction *f* with increasing liver fibrosis suggests that the observed corresponding *ADC* decreases are due to anticipated blood flow alterations with progressive disease. Liver fibrosis involves the excessive accumulation of extracellular matrix proteins, including collagen and fibrous scar tissue. In prior CCl_4 rodent studies of Annet et al(15), a decrease of *ADC* with increasing fibrosis level was observed only in living animals; a proposed possible explanation is that a decrease in perfusion caused this decrease in *ADC*. This explanation is in agreement with the patient studies of Luciani et al (14) in which the calculated perfusion component (D^*) significantly decreases in the a cirrhotic liver group compared with D^* measured within healthy liver tissues.

Presently liver biopsy is the gold standard for detection and staging of liver fibrosis. However, a limitation of biopsy procedures is that these are invasive and have sampling errors and a high rate of complications due to the procedure (7, 26). Meanwhile, other noninvasive diagnostic methods have been developed for the detection of liver fibrosis. Ultrasonographic diagnosis(27), transient sonoelastography(28), computed tomography(29) and dynamic contrast-enhanced (DCE) MRI, MR elastography(30) and DW MRI(31) have been proposed for noninvasive diagnosis and staging of liver fibrosis. Timing bolus DCE

MRI has been used to obtain hepatic perfusion parameters for differentiating patients with and without cirrhosis(32). However, the intravenous injection of contrast agents is required for quantitative DCE. The requirement of IV contrast can severely limit the utility of this technique due to a vast majority of patients suffering from renal insufficiency, which limits our ability to use IV contrast agents. Recently, carbogen gas-challenge BOLD MRI was proposed to correlate gas-challenge BOLD response (33) with the degree of liver fibrosis, in which a significant inverse correlation was observed (34). Our current results in the diethylnitrosamine-treated rodent model suggest that the use of IVIM approaches might offer a promising non-invasive method for the diagnosis of liver fibrosis and functional assessment of hepatic perfusion. Further studies are necessary to fully characterize the sensitivity and specificity of IVIM methods for staging disease progression.

In conclusion, the hepatic ADC and the perfusion fraction f decreased significantly with the liver fibrosis level in the Wistar rat. The correlation between the true diffusion value D and the fibrosis level was not observed. These measurements suggest that perfusion changes during the progression of hepatic fibrosis and can be easily detected using IVIM.

Acknowledgments

Funding Information: This publication was made possible by Grant Number NIH R01 CA126809-01A2 and R01 CA134719-01. The authors wish to acknowledge the SIR Foundation and the Rosenberg Family Cancer Research Fund (RFCRF). Its contents are solely the responsibility of the authors and do not necessarily represent the official view of NIH, SIR or RFCRF.

REFERENCES

1. Schuppan D, Popov Y. Hepatic fibrosis: from bench to bedside. J Gastroenterol Hepatol. 2002; 17(Suppl 3):S300–S305. [PubMed: 12472954]
2. Friedman SL. Liver fibrosis -- from bench to bedside. Journal of hepatology. 2003; (Suppl 1):S38–S53. [PubMed: 12591185]
3. Williams R. Global challenges in liver disease. Hepatology (Baltimore, Md. 2006; 44(3):521–526.
4. Proceedings of the European Association for the Study of the Liver (EASL) International Consensus Conference on Hepatitis B. September 14–16, 2002. Geneva, Switzerland. Journal of hepatology. 2003; 39(Suppl 1):S1–S235. [PubMed: 14964189]
5. Poynard T, Bedossa P, Opolon P. Natural history of liver fibrosis progression in patients with chronic hepatitis C. The OBSVIRC, METAVIR, CLINIVIR, and DOSVIRC groups. Lancet. 1997; 349(9055):825–832. [PubMed: 9121257]
6. Dienstag JL. The role of liver biopsy in chronic hepatitis C. Hepatology (Baltimore, Md. 2002; 36(5 Suppl 1):S152–S160.
7. Afdhal NH, Nunes D. Evaluation of liver fibrosis: a concise review. The American journal of gastroenterology. 2004; 99(6):1160–1174. [PubMed: 15180741]
8. Aube C, Racineux PX, Lebigot J, et al. Diagnosis and quantification of hepatic fibrosis with diffusion weighted MR imaging: preliminary results. Journal de radiologie. 2004; 85(3):301–306. [PubMed: 15192522]
9. Lewin M, Poujol-Robert A, Boelle PY, et al. Diffusion-weighted magnetic resonance imaging for the assessment of fibrosis in chronic hepatitis C. Hepatology (Baltimore, Md. 2007; 46(3):658–665.
10. Le Bihan D, Breton E, Lallemand D, Aubin ML, Vignaud J, Laval-Jeantet M. Separation of diffusion and perfusion in intravoxel incoherent motion MR imaging. Radiology. 1988; 168(2): 497–505. [PubMed: 3393671]
11. Turner R, Le Bihan D, Maier J, Vavrek R, Hedges LK, Pekar J. Echo-planar imaging of intravoxel incoherent motion. Radiology. 1990; 177(2):407–414. [PubMed: 2217777]
12. Le Bihan D, Breton E, Lallemand D, Grenier P, Cabanis E, Laval-Jeantet M. MR imaging of intravoxel incoherent motions: application to diffusion and perfusion in neurologic disorders. Radiology. 1986; 161(2):401–407. [PubMed: 3763909]

13. Annet L, Materne R, Danse E, Jamart J, Horsmans Y, Van Beers BE. Hepatic flow parameters measured with MR imaging and Doppler US: correlations with degree of cirrhosis and portal hypertension. Radiology. 2003; 229(2):409–414. [PubMed: 12970464]
14. Luciani A, Vignaud A, Cavet M, et al. Liver cirrhosis: intravoxel incoherent motion MR imaging--pilot study. Radiology. 2008; 249(3):891–899. [PubMed: 19011186]
15. Annet L, Peeters F, Abarca-Quinones J, Leclercq I, Moulin P, Van Beers BE. Assessment of diffusion-weighted MR imaging in liver fibrosis. J Magn Reson Imaging. 2007; 25(1):122–128. [PubMed: 17154179]
16. Yamada I, Aung W, Himeno Y, Nakagawa T, Shibuya H. Diffusion coefficients in abdominal organs and hepatic lesions: evaluation with intravoxel incoherent motion echo-planar MR imaging. Radiology. 1999; 210(3):617–623. [PubMed: 10207458]
17. Girometti R, Furlan A, Esposito G, et al. Relevance of b-values in evaluating liver fibrosis: a study in healthy and cirrhotic subjects using two single-shot spin-echo echoplanar diffusion-weighted sequences. J Magn Reson Imaging. 2008; 28(2):411–419. [PubMed: 18666139]
18. Steinhoff D. Effect of diethylnitrosamine on the livers of rats after high oral doses administered at intervals varying between three and twenty-four days. Acta Hepatogastroenterol (Stuttg). 1975; 22(2):72–77. [PubMed: 165650]
19. Patel J, Sigmund EE, Rusinek H, Oei M, Babb JS, Taouli B. Diagnosis of cirrhosis with intravoxel incoherent motion diffusion MRI and dynamic contrast-enhanced MRI alone and in combination: preliminary experience. J Magn Reson Imaging. 2010; 31(3):589–600. [PubMed: 20187201]
20. Vyvenko OF. Exponential analysis in physical phenomena. Review of Scientific Instruments. 1999; 70(2)
21. Yao L, Sinha U. Imaging the microcirculatory proton fraction of muscle with diffusion-weighted echo-planar imaging. Acad Radiol. 2000; 7(1):27–32. [PubMed: 10645455]
22. Wirestam R, Borg M, Brockstedt S, Lindgren A, Holtas S, Stahlberg F. Perfusion-related parameters in intravoxel incoherent motion MR imaging compared with CBV and CBF measured by dynamic susceptibility-contrast MR technique. Acta Radiol. 2001; 42(2):123–128. [PubMed: 11281143]
23. Callot V, Bennett E, Decking UK, Balaban RS, Wen H. In vivo study of microcirculation in canine myocardium using the IVIM method. Magn Reson Med. 2003; 50(3):531–540. [PubMed: 12939761]
24. Muskopf, S. Rat Dissection Step 6. Available at: http://www.biologycorner.com/worksheets/rat_dissection06.html. Accessed.
25. Masseroli M, Caballero T, O'Valle F, Del Moral RM, Perez-Milena A, Del Moral RG. Automatic quantification of liver fibrosis: design and validation of a new image analysis method: comparison with semi-quantitative indexes of fibrosis. Journal of hepatology. 2000; 32(3):453–464. [PubMed: 10735616]
26. Wong JB, Bennett WG, Koff RS, Pauker SG. Pretreatment evaluation of chronic hepatitis C: risks, benefits, and costs. Jama. 1998; 280(24):2088–2093. [PubMed: 9875876]
27. Aube C, Oberti F, Korali N, et al. Ultrasonographic diagnosis of hepatic fibrosis or cirrhosis. Journal of hepatology. 1999; 30(3):472–478. [PubMed: 10190731]
28. Sandrin L, Fourquet B, Hasquenoph JM, et al. Transient elastography: a new noninvasive method for assessment of hepatic fibrosis. Ultrasound in medicine & biology. 2003; 29(12):1705–1713. [PubMed: 14698338]
29. Romero-Gomez M, Gomez-Gonzalez E, Madrazo A, et al. Optical analysis of computed tomography images of the liver predicts fibrosis stage and distribution in chronic hepatitis C. Hepatology (Baltimore, Md. 2008; 47(3):810–816.
30. Muthupillai R, Ehman RL. Magnetic resonance elastography. Nature medicine. 1996; 2(5):601–603.
31. Koinuma M, Ohashi I, Hanafusa K, Shibuya H. Apparent diffusion coefficient measurements with diffusion-weighted magnetic resonance imaging for evaluation of hepatic fibrosis. J Magn Reson Imaging. 2005; 22(1):80–85. [PubMed: 15971188]

32. Baxter S, Wang ZJ, Joe BN, Qayyum A, Taouli B, Yeh BM. Timing bolus dynamic contrast-enhanced (DCE) MRI assessment of hepatic perfusion: Initial experience. J Magn Reson Imaging. 2009; 29(6):1317–1322. [PubMed: 19472388]

33. Barash H, Gross E, Edrei Y, et al. Functional magnetic resonance imaging monitoring of pathological changes in rodent livers during hyperoxia and hypercapnia. Hepatology (Baltimore, Md. 2008; 48(4):1232–1241.

34. Jin N, Deng J, Chadashvili T, et al. Carbogen gas-challenge BOLD MR imaging in a rat model of diethylnitrosamine-induced liver fibrosis. Radiology. 2010; 254(1):129–137. [PubMed: 20032147]

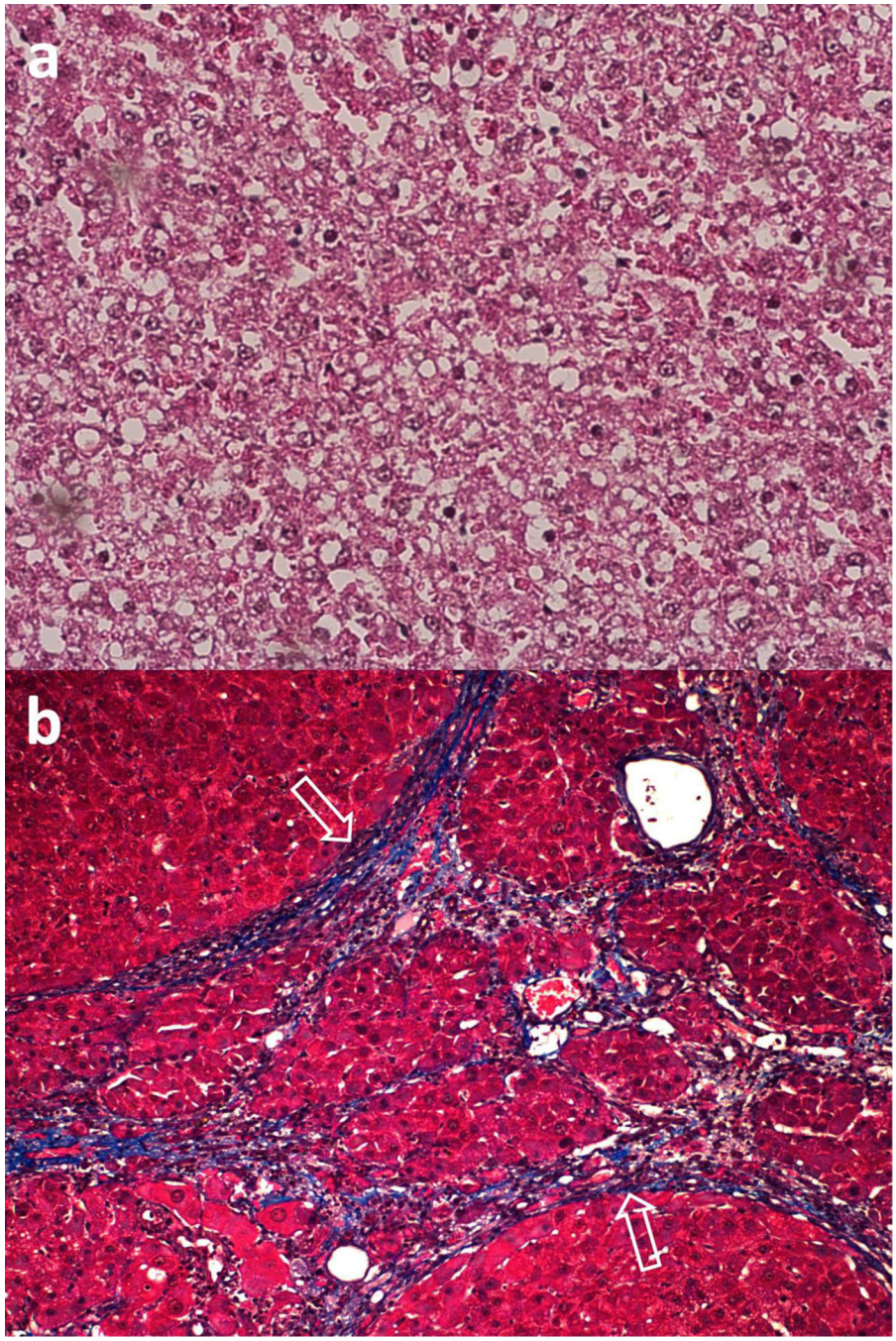

Figure 1.
Masson trichrome histological slides of rat liver tissues. Healthy control rats showed no fibrosis (**a**) whereas DEN-induced fibrosis rats (**b**) demonstrated significant levels of fibrotic tissue (white arrows).

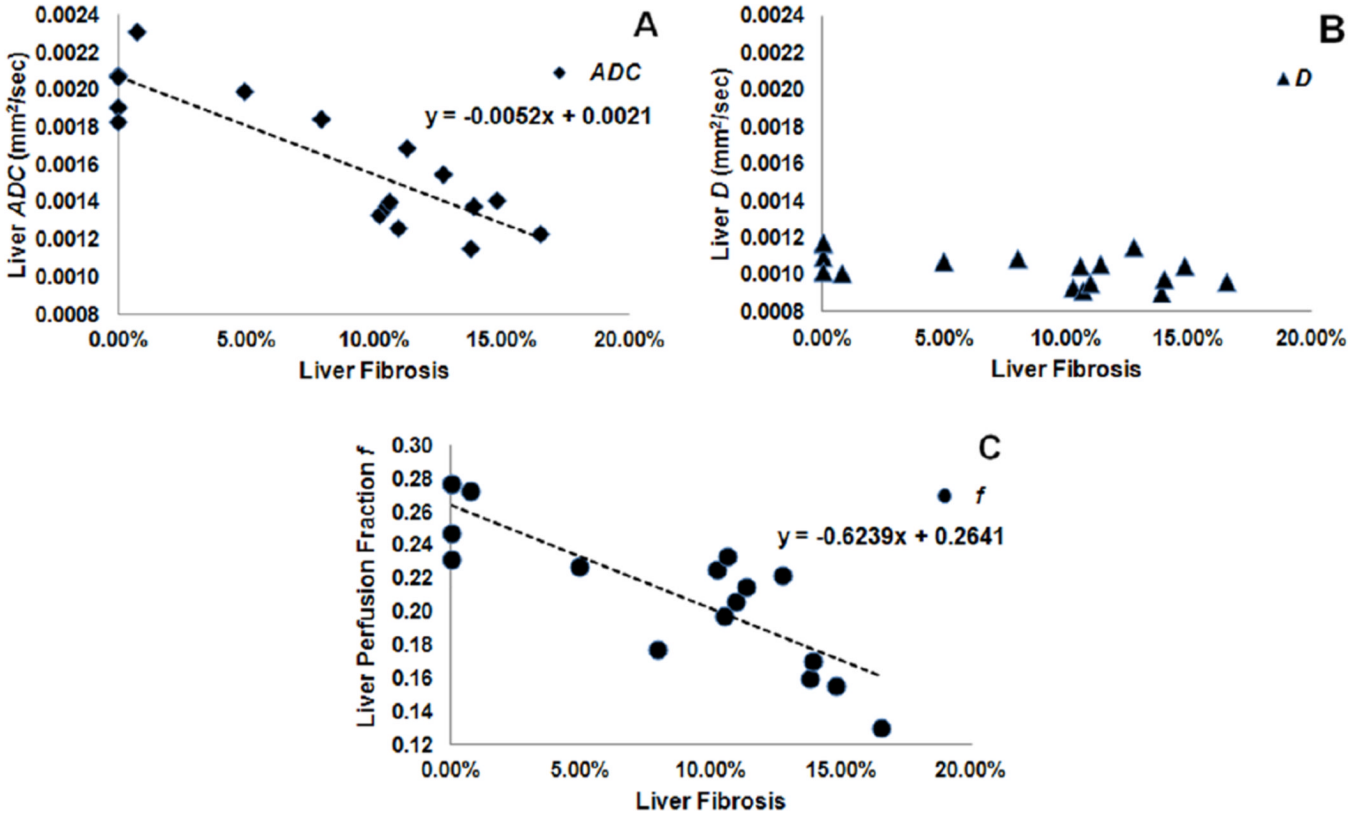

Figure 2.

Scatter-plots comparing liver *ADC* (a), diffusion *D* (b) and *f* (c) measurements in ROI to percent fibrosis levels in 17 DEN-induced fibrosis rats. A significant inverse correlation was observed for *ADC* ($\rho = -0.781$, $p < 0.001$) and *f* ($\rho = -0.720$, $p = 0.001$). D was poorly correlated ($\rho = -0.502$, $p = 0.040$) with fibrosis level.

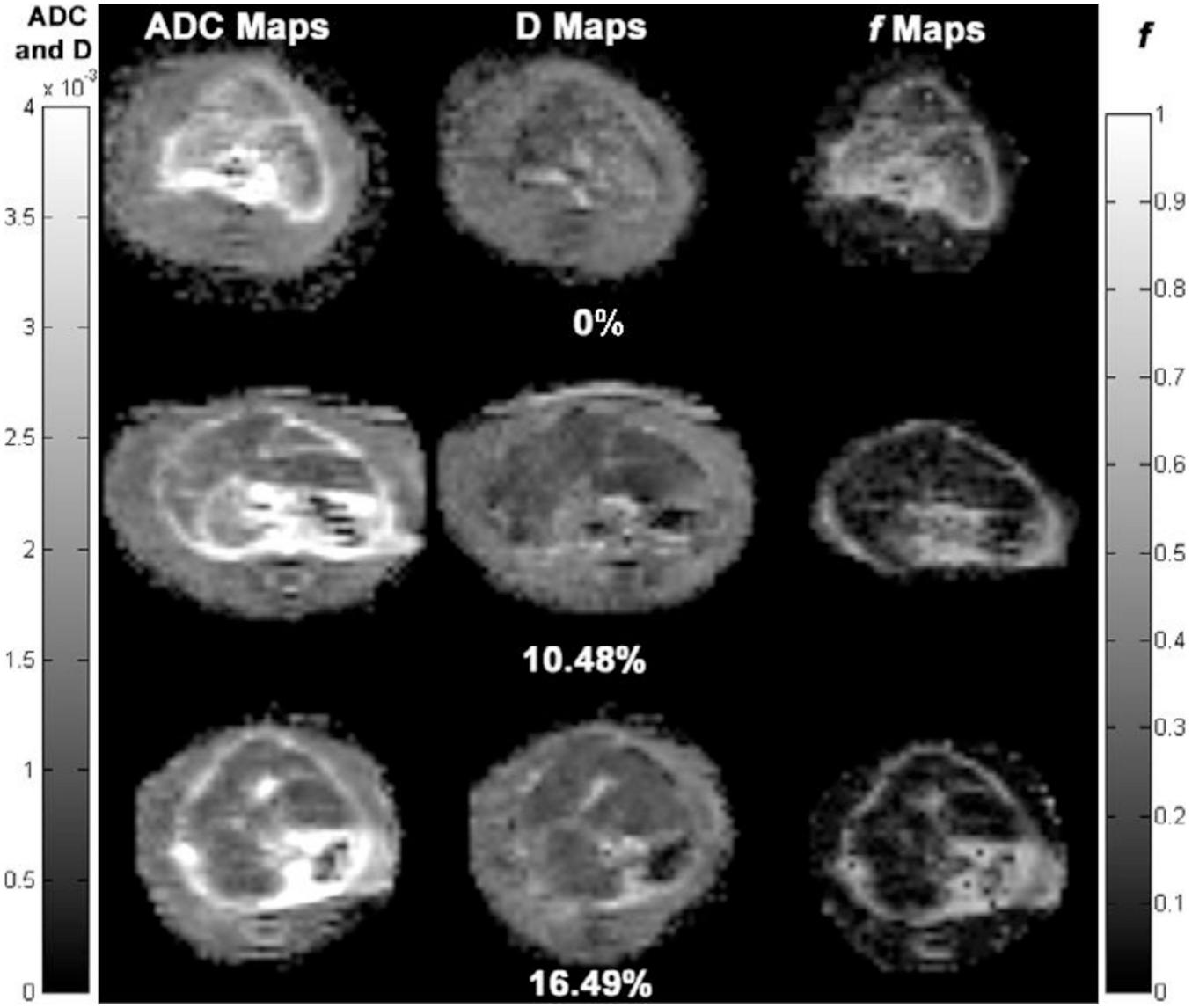

Figure 3.

Representative axial *ADC*, *D* (true diffusion coefficient) and *f* (perfusion fraction) maps of Wistar rat livers at different fibrosis degrees (0%, 10.48% and 16.49%). The hepatic *ADC* and *f* values of 0% fibrosis (brighter on ADC and *f* maps) were higher than that of 10.48% and 16.49% fibrosis (darker on ADC and *f* maps), while hepatic *D* values were similar in the three levels of fibrosis. Left grey scale indicated values for *ADC* and *D* maps. Right grey scale indicated values for *f* maps.